Elastically Adaptive Deformable Models

Dimitris N. Metaxas, *Senior Member*, *IEEE*, and Ioannis A. Kakadiaris, *Member*, *IEEE*

Abstract—We present a novel technique for the automatic adaptation of a deformable model's elastic parameters within a Kalman filter framework for shape estimation applications. The novelty of the technique is that the model's elastic parameters are not constant, but spatio-temporally varying. The variation of the elastic parameters depends on the distance of the model from the data and the rate of change of this distance. Each pass of the algorithm uses physics-based modeling techniques to iteratively adjust both the geometric and the elastic degrees of freedom of the model in response to forces that are computed from the discrepancy between the model and the data. By augmenting the state equations of an extended Kalman filter to incorporate these additional variables, we are able to significantly improve the quality of the shape estimation. Therefore, the model's elastic parameters are always initialized to the same value and they are subsequently modified depending on the data and the noise distribution. We present results demonstrating the effectiveness of our method for both two-dimensional and three-dimensional data.

Index Terms—Adaptive elastic parameters, deformable models, shape estimation, physics-based modeling, Kalman filter.

1 Introduction

There are several applications where accurate shape estimation is desired while the shape characteristics of the data may vary significantly in space and/or time. Such applications include accurate contour estimation from biomedical data and the extraction of 3D shape from range data. In all these applications, minimal human intervention in terms of defining the model's initial parameters is desired.

Deformable model formulations provide a powerful mechanism for quantitatively modeling and analyzing an object's shape, structure and motion [1], [6], [8], [9], [12], [14], [16], [17], [15], [18], [21], [36], [31], [30], [32], [33], [35], [37], [40], [44], [53], [54], [56]. Deformable models offer a data-driven recovery process, in which forces derived from the image deform the model until it fits the data. However, most such formulations assume that the user correctly initializes the model's elastic parameters which significantly affect the goodness of fit of the model to the given data. For example, in [31], it was assumed that the elastic parameters of the finite elements used for shape estimation remain constant in space and, in time, and that the user chooses the initial values. However, the speed and accuracy of fitting the models to the data depends on the values selected for the elastic parameters of the model. This is a significant limitation in model fitting applications where the user assumes no a priori knowledge of the complexity of the given data.

In this paper, we propose a new formal methodology to automatically determine a deformable model's elastic parameters which generalizes our previous formulation [31]. According to our deformable model framework, the surface of the model is tessellated into a grid of finite elements. Each finite element has its own elastic parameters and these parameters may vary in time during the fitting. The technique that we are presenting is based on the use of a model for the adaptation of the model's elastic parameters. The characteristic of this method is that each elastic parameter is modified based on the local distance of the model from the data and the local rate of change of this distance. If the model's initial elastic parameters are sufficient to fit the given data within a user specified tolerance, then their change during the fitting process will be minimal. Otherwise, they will gradually change based on the above criteria. In particular, the elastic parameters decrease when the model has not fit the data to make the model more elastic and allow for fitting. On the contrary, when the model is close to the data the elastic parameters increase to make the model more stiff. This increase of the elastic parameters has the effect of anchoring the model to the portion of the data it has fit and also improves the continuity of the solution.

Based on our previous experience with incorporating a dynamic deformable model into an extended Kalman filter framework, we develop a *modified* extended Kalman filter. This filter allows the simultaneous modification of the model's degrees of freedom and its elastic parameters. In particular, we extend the state vector of the dynamical system which corresponds to our deformable model, to include the model's elastic parameters. This modification is based on the theory of dynamic system parameter identification [11]. We present a series of experiments with two- and three-dimensional data to demonstrate the effectiveness of our technique in accurate shape estimation, where the elastic parameters are always initialized to the same value.

The rest of the paper is organized as follows:[1] Section 2 presents previous research related to the new technique. Section 3 reviews the formulation of deformable models. Section 4 presents the new technique for the spatio-temporal adaptation of the elastic parameters of a deformable model. Section 5 presents the incorporation of the elastic parameters into an extended Kalman filter formulation. Section 5.1 demonstrates how this technique can be parallelized in order to increase its efficiency. Finally, the effectiveness of the

- *D.N. Metaxas is with the Division of Computer and Information Sciences, Rutgers The State University of New Jersey, 110 Frelinghuysen Road, Piscataway, NJ 08854-8019. E-mail: dnm@cs.rutgers.edu.*
- *I.A. Kakadiaris is with the Department of Computer Science, MS CSC 3010, University of Houston, 4800 Calhoun, Houston, TX 77204-3010. E-mail: ioannisk@uh.edu.*

Manuscript received 14 Mar. 1998; revised 1 July 2001; accepted 25 Sept. 2001.
Recommended for acceptance by Y.-F. Wang.
For information on obtaining reprints of this article, please send e-mail to: tpami@computer.org, and reference IEEECS Log Number 107636.

1. Parts of this paper have appeared previously in [29].

approach is demonstrated through a series of experiments in Section 6.

2 Related Work

Curve/surface reconstruction has been a topic of extensive interest, involving the estimation of an unknown curve/surface based on a set of noisy measurements of a function of the curve/surface [5], [23], [24], [41], [45], [46], [50], [51], [49], [48], [39]. Several variational shape reconstruction methods have been proposed to address the problem of fitting noisy data [42], [22], [3]. Variational methods minimize a (possibly nonconvex) energy functional. To efficiently achieve a significant optimum for the nonconvex optimization a coarse to fine scale space tracking technique was proposed in [55]. In this approach, the desired solution is obtained by first finding a solution at a significantly coarser scale and then tracking it down through finer scales. Empirical evidence suggests that this technique can find useful significant minima that exist over a large range of scale. Fitting of noisy data can be accomplished also using smoothing splines, where a smoothing parameter is used to control the tradeoff between the closeness and smoothness of fit [52]. An "optimal" smoothing parameter can be estimated, for example, by cross-validation [52]. The dynamic form of the deformable model fitting technique was first introduced by Kass et al. [19]. They proposed a dynamic deformable cylinder model constructed from generalized splines [2], [43], along with force-based techniques to fit the model to image data. Most deformable model shape recovery algorithms [6], [7], [19], [26], [31], [30], [31], [34], [38], [44], [57] assume that the user correctly initializes the model's parameters which determine the goodness of fit of the model to the given data. Recently, there have been several attempts to overcome the above problem for the case of two-dimensional models only [1], [35], [21], [20]. Blake and Isard [1] developed a new technique based on ideas from adaptive control theory and maximum-likelihood estimation, to learn the model dynamics for tracking in real time 2D curve motions similar to those in the training set. However, the method is most useful when used for the estimation of classes of objects for which training data is available from objects within that particular class. Samadani [35] provides rules to estimate and adjust the parameters of a snake to avoid instabilities and improve the accuracy of shape estimation. Larsen et al. [21], [20] develops a formalism by which an estimate for the upper and lower bounds on the elasticity parameters of a snake can be obtained. However, the analysis requires knowledge of the shape of the object of interest and applies to two-dimensional models only. Contrary to many of the above techniques, our proposed method provides an efficient and intuitive way to automatically adapt the elastic parameters of a deformable model.

Kalman filtering methods have also been used by many researchers in computer vision to account for noise in the data [1], [4], [8], [25], [27], [34]. As opposed to previous Kalman filter formulations for deformable models, we use notions from parameter identification theory to incorporate the model's elastic parameters into a Kalman Filter. This is necessary because these parameters are not explicitly part of the model's state (see Section 3). In this paper, we do not address the issue of multilevel shape representation using locally adaptive finite elements [30], [47]. However, the method presented can be used in conjunction with these methods to further improve the shape estimation results.

3 Deformable Model Geometry: A Review

We briefly review the notation for deformable models [31], [44]. The models used in this work are two- and three-dimensional. The material coordinates $\mathbf{u}$ ($\mathbf{u} = (v)$ and $\mathbf{u} = (u, v)$ for the two-and three-dimensional case, respectively) of a point on these models are specified over a domain Ω. The position of a point on the model relative to an inertial frame of reference Φ in space is given by a vector-valued, time varying function. In particular, the three-dimensional position of a point with respect to (w.r.t.) a world coordinate system is the result of the translation and rotation of its position with respect to a noninertial, model-centered coordinate frame ϕ (Fig. 1). Therefore, the position of a point (with material coordinates $\mathbf{u}$) on a deformable model at time t with respect to an inertial frame of reference Φ is given by the formula:

$$^{\Phi}\mathbf{x}(\mathbf{u}, t) = {}^{\Phi}\mathbf{t}(t) + {}^{\Phi}_{\phi}\mathbf{R}(t)\,{}^{\phi}\mathbf{p}(\mathbf{u}, t), \tag{1}$$

where ${}^{\Phi}\mathbf{t}$ is the position of the origin O of the model frame ϕ with respect to the frame Φ (the model's translation), and ${}^{\Phi}_{\phi}\mathbf{R}$ is the matrix that encapsulates the orientation of ϕ with respect to Φ. To introduce global and local deformations, the position of a model point with material coordinate $\mathbf{u}$ w.r.t. the model frame ${}^{\phi}\mathbf{p}(\mathbf{u}, t)$ is expressed as the sum of a reference shape ${}^{\phi}\mathbf{s}(\mathbf{u}, t)$ and a local displacement ${}^{\phi}\mathbf{d}(\mathbf{u}, t)$ as given by the formula:

$$^{\phi}\mathbf{p}(\mathbf{u}, t) = {}^{\phi}\,\mathbf{s}(\mathbf{u}, t) + {}^{\phi}\,\mathbf{d}(\mathbf{u}, t). \tag{2}$$

The reference shape captures the salient shape features of the model and it is the result of applying global deformation function $\mathbf{T}$ (such as tapering and bending) to a geometric primitive $\mathbf{e} = (e_x, e_y, e_z)^{\top}$. In particular,

$$^{\phi}\mathbf{s}(v, t) = (s_x, s_y, s_z)^{\top} = \mathbf{T}(\mathbf{e}; \mathbf{q}_T), \tag{3}$$

where the global deformations defined by $\mathbf{T}$ depend on the parameters $\mathbf{q}_T$. In this paper, we employ a superellipsoid $\mathbf{e}(v)[-\pi, \pi) \rightarrow \mathbb{R}^2$ with global shape parameters $\mathbf{q}_{\mathbf{e}} = (\alpha_1, \alpha_2, \beta_1)^{\top}$ as a two-dimensional shape primitive. As a three-dimensional shape primitive, we employ a superquadric $\mathbf{e}(u, v) : [-\frac{\pi}{2}, \frac{\pi}{2})\mathrm{x}[-\pi, \pi) \rightarrow \mathbb{R}^3$ with global shape parameters $\mathbf{q}_{\mathbf{e}} = (\alpha_1, \alpha_2, \alpha_3, \beta_1, \beta_2)^{\top}$, where $\alpha_1, \alpha_2, \alpha_3 \geq 0$ are the parameters that define the superquadric size, and β_1 and β_2 are the "squareness" parameters in the latitude and longitude plane, respectively. We employ the finite element method to represent the continuous surface of the deformable model in the form of weighted sums of local polynomial basis functions. The finite element method provides an analytic, piecewise polynomial surface representation. Local displacements $\mathbf{d}$ are computed based on the use of triangular finite elements. Associated with every finite element node i is a nodal vector variable $\mathbf{q}_{d,i}$. We collect all the nodal variables into a vector of local degrees of freedom $\mathbf{q}_d = (\ldots, \mathbf{q}_{d,i}^{\top}, \ldots)^{\top}$ and we compute the local displacement $\mathbf{d}$ based on the finite element theory as $\mathbf{d} = \mathbf{S}\mathbf{q}_d$. $\mathbf{S}$ is the shape matrix whose entries are the finite element shape functions. Finally, we incorporate into the vector $\mathbf{q} = (\mathbf{q}_c^{\top}, \mathbf{q}_{\theta}^{\top}, \mathbf{q}_s^{\top}, \mathbf{q}_d^{\top})^{\top}$ the degrees of freedom of our model which consist of the parameters

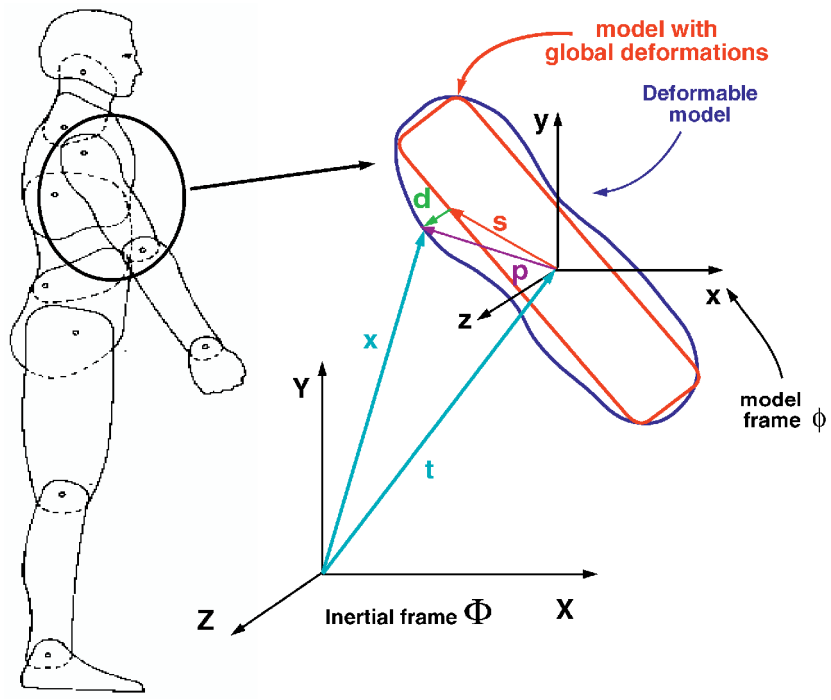

Fig. 1. Coordinate systems for deformable models.

necessary to define the translation $\mathbf{q}_c$, rotation $\mathbf{q}_\theta$, global $\mathbf{q}_s$ and local deformations $\mathbf{q}_d$ of the model [44]. Our goal when fitting the model to the data is to recover the vector of degrees of freedom $\mathbf{q}$. This is achieved in a physics-based way [28]. We assume that the model is composed from simulated elastic material. According to the physics-based framework, the image data apply simulated forces to the points in the model. Responding to the external forces, the model moves and deforms to fit the data. The molding of the model through time can be described in the terms of differential equations which can be numerically solved to estimate the shape parameters of the object under observation. The formulation of the motion equations includes a strain energy and simulated forces. Deformation results from the action of internal forces, which impose surface continuity constraints, and the external forces from the data to the surface of the model. In particular, the simplified equations of motion [31] that we use take the general form

$$\mathbf{D}\dot{\mathbf{q}} + \mathbf{K}\mathbf{q} = \mathbf{f}_q, \tag{4}$$

where $\mathbf{f}_q$ are the generalized external forces computed from the 2D or 3D forces applied from the data to the model (more details on the computation of the generalized forces are provided in [44]), $\mathbf{K}$ is the stiffness matrix, and $\mathbf{D}$ is the damping matrix.

4 Adaptive Elastic Parameters

A dynamic deformable model has kinetic energy and deformation strain energy $\mathcal{E}$. The strain term directly parallels the smoothness functional employed in regularization [42]. In particular, the deformation energy that we impose upon the model depends on the desired continuity for the deformable model. According to the theory of elasticity, the relationship between the stresses (σ) and strains (ϵ) of an elastic material is expressed as

$$\sigma = \frac{d\mathcal{E}}{d\epsilon} = \mathbf{C}\epsilon \tag{5}$$

for a linear material and as

$$d\sigma = \mathbf{C}(\epsilon)d\epsilon \tag{6}$$

for a nonlinear material. Furthermore, by assuming a small stress-strain displacement[2] and the use of finite elements, we can take it one step further to:

$$\epsilon = \mathbf{P}\mathbf{d} = \mathbf{P}\mathbf{S}\mathbf{q}_d, \tag{7}$$

where $\mathbf{d}$ is the material displacement, $\mathbf{S}$ is the finite element shape matrix, $\mathbf{q}_d$ are the FEM nodal displacements, and the symmetric matrix $\mathbf{P}$ is derived from the local deformation strain energy. Based on the above definitions and the theory of elasticity, we can express the (linear or nonlinear) elastic deformation energy $\mathcal{E}$ w.r.t. to the FEM coordinates as

$$\mathcal{E} = \int \epsilon^\top \sigma \, d\mathrm{u} = \mathbf{q}_d^\top \left[\int (\mathbf{PS})^\top \mathbf{C}(\epsilon)(\mathbf{PS}) \, d\mathrm{u} \right] \mathbf{q}_d, \tag{8}$$

where the stiffness matrix $\mathbf{K}$ is defined as

$$\mathbf{K} = \int (\mathbf{PS})^\top \mathbf{C}(\epsilon)(\mathbf{PS}) \, d\mathrm{u}. \tag{9}$$

In the past, we have used a combined membrane and thin plate deformation energy which can be written in the general form:

$$\mathcal{E} = \frac{1}{2} \int \left(w_1 \epsilon_{11}^2 + w_2 \epsilon_{22}^2 + w_3 \epsilon_{33}^2 + w_4 \epsilon_{12}^2 + w_5 \epsilon_{23}^2 + w_6 \epsilon_{13}^2 \right) d\mathrm{u}, \tag{10}$$

2. The theory easily generalizes to large stress-strains [58].

where ϵ_{ij} are the components of the strain vector ϵ. The nonnegative weighting functions w_i control the elasticity of the material.

Most finite element implementations for computer vision applications, assume that the elastic parameters w_i are constant across the deformable model and during the model fitting process. They are also initialized manually in the beginning of the shape estimation process. This may result in lengthy manual experimentations to identify the correct initial elastic parameter values. Second, since these parameters are assumed constant across the model, accurate shape estimation may never be achieved in case of complex data. Clearly, a technique for automatically adjusting a deformable model's elastic parameters in a local fashion is necessary.

The first contribution of this paper is the development of a new method for automatically modifying the elastic parameters w_i for each of the model's finite elements. The model for the modification of each of the model's elastic parameters is based on ideas from the theory of PD (Proportional-Derivative) control. In particular, the model's elastic parameters are modified during the fitting process based on the local distance of the model from the data and the rate of change of this distance. In all of the experiments, we start the fitting process with the same initial value $w_0 = 0.005$ for all the model's elastic parameters. In our implementation, each finite element j, $(j = 1, \ldots, k)$, where k is the number of finite elements of the model, has its own elastic parameters $w_i^j (i = 1, \ldots, 6)$. The fitting of the deformable model to the given data is based on (4). For each finite element j, the average distance to the data ψ^j is defined as:

$$\psi^j = \frac{\sum_{k=1}^{m} \phi_k^j}{m},$$

where ϕ_k^j is the normalized average distance from the data of each of the nodes k of the finite element j and m is the number of nodes of finite element j. The normalized average distance ϕ_k^j is defined to be the average distance of a node of the model from the data normalized by the fitting error tolerance ψ_{tot} ($\psi_{tol} \neq 0$) as follows:

$$\phi_k^j = \frac{\sum_{l=1}^{p} \left(\frac{\boldsymbol{\rho}_l - \mathbf{x}_k^j}{\psi_{tol}} \right)}{p}, \tag{11}$$

where $\mathbf{x}_k^j$ is the position of the kth node of element j and $\boldsymbol{\rho}_l$ is the position of the lth data point from the p data points that have been assigned to the kth node according to any of the schemes defined in [27]. During the fitting process, the values of each of the elastic parameters w_i^j for each finite element j are modified based on

$$w_i^j(t) = (w_0 - w_{min}) \; e^{sgn\left(\psi^j \cdot \dot{\psi}^j\right)\left(||\psi^j|| + ||\dot{\psi}^j||\right)} + w_{min}, \tag{12}$$

where w_{min} is the minimum value for all the elastic parameters, which for a membrane and/or thin-plate deformable model was experimentally selected to be $5 \cdot 10^{-4}$, and sgn is the $sign$ function. Note that the success of our technique depends on the selection of the value w_{min}. Notice that $sgn(\psi^j \cdot \dot{\psi}^j)$ is negative or zero when the model is converging towards the data and positive otherwise. The whole process of fitting and elastic parameter adaptation terminates when the distance of the model from the data for each finite element is below a tolerance ψ_{tol} specified by the user.

The adaptation of the elastic parameters of a deformable model using the method described above has the following desired properties. As seen in (12), the change in each of the w_i^js is always w.r.t. their initial value w_0. Initially, since the distance of the model from the data is large, while the rate of change of this distance is small or zero, the values of the w_i^js decrease exponentially to quickly improve the fitting. In the intermediate steps of the fitting, the values of the w_i^js stabilize and are not modified significantly since the sum of the distance of the model from the data and the rate of change of this distance does not change substantially. When the model is very close to the desired data, the sum of this distance and its rate of change decrease (the forces assigned to each node are now small) and the result is an increase of the w_i^js towards w_0. (See Fig. 8.) This results in a model that achieves a solution with C^1 continuity where necessary and also better "holds" the model to the desired data. When the model has almost fit the data, the values of the w_i^js start to exponentially increase again towards their initial value. Therefore, the elastic parameters oscillate mostly between w_0 and w_{min}. Due to the introduction of $sgn(\psi^j \cdot \dot{\psi}^j)$ in (12), the model's elastic parameters are automatically increased beyond w_0 if the model has fit the data and tries to deviate from them. Therefore, the model resists deviation from the data once it has fit them. This is an additional desired property in cases where the model has partially fit the data. It will allow the portion of the model that has not fit the data to become more elastic and fit the data, while the portion that has fit them will either not be modified or become more stiff in case there is any deviation from the data.

5 Dynamic Shape Estimation

The above model for the modification of the model's elastic parameters does not take into account the noise in the data. In [27], it was shown how the dynamics of a deformable model can be incorporated into an extended Kalman filtering framework to formally account for noise in the data. However, an extension to this formulation is necessary in order to incorporate the model for the modification of the model's elastic parameters into a Kalman filter. This is necessary because the model's elastic parameters are not degrees of freedom, since they do not appear in $\mathbf{q}$, but are the unknown parameters that determine the value of the stiffness matrix $\mathbf{K}$. Therefore, this problem is that of parameter identification in a dynamic system. In [10], [11], the theory of parameter identification in dynamic systems is presented. Based on this approach, with the addition that we have a model for the modification of the deformable model's elastic parameters,[3] we augment the state vector of our system to include the model's elastic parameters. Therefore, the new state vector is of the form

$$\mathbf{b} = \begin{bmatrix} \mathbf{w} \\ \mathbf{q} \end{bmatrix}, \tag{13}$$

where $\mathbf{w}$ is the vector of the model's elasticity parameters with components w_i^j.

3. According to that theory, the time derivative of the elastic parameters should have been zero as opposed to the one used herein.

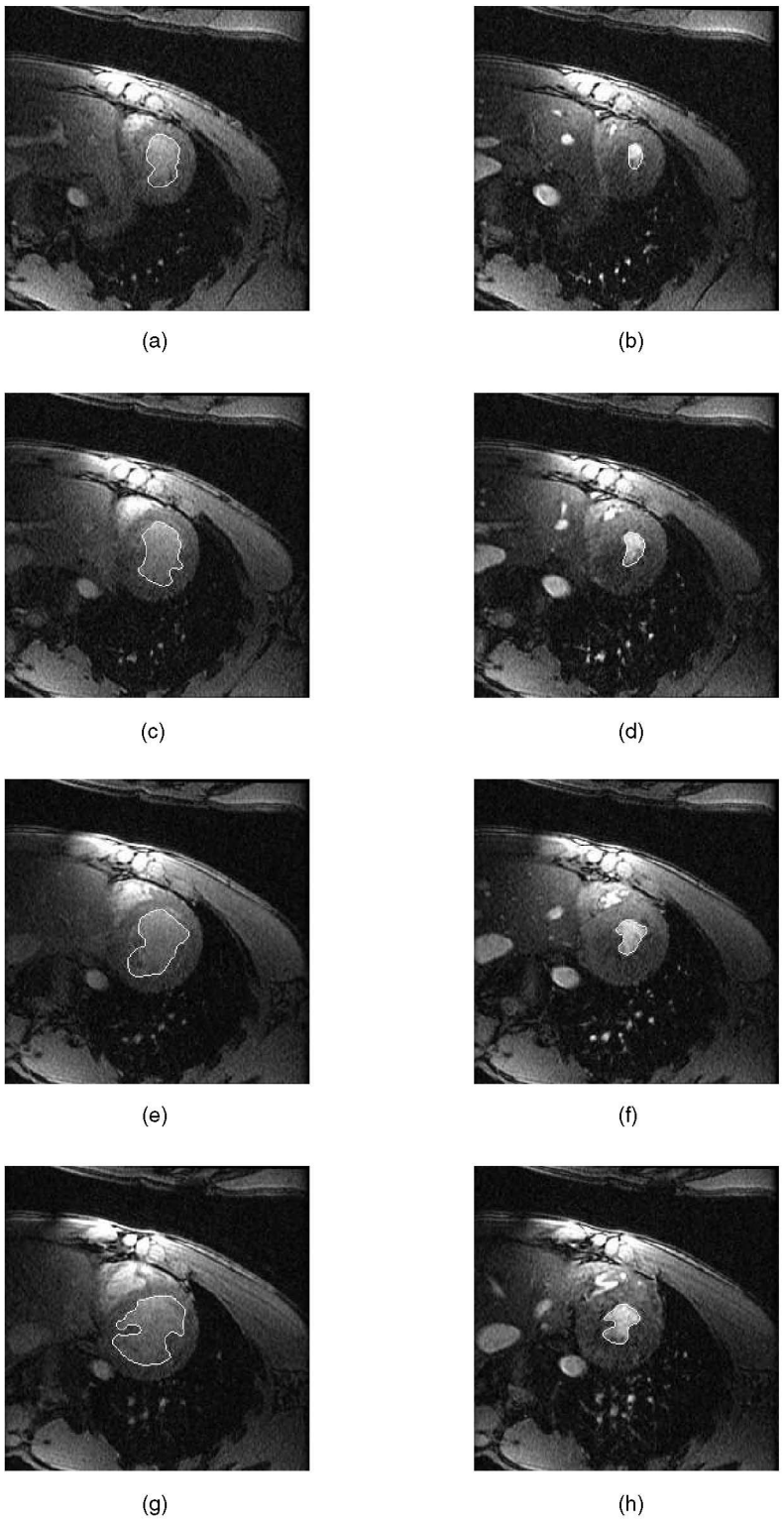

Fig. 2. Semiautomated identification of the myocardial borders. (a), (c), (e), and (g) End diastole phase, and (b), (d), (f), and (h) end systole phase for locations 4, 5, 6, and 7, respectively.

Based on the above modification, we introduce the following definitions necessary to define the equations of a modified extended Kalman filter. Let the observation vector $\mathbf{z}(t)$ denote time-varying input data. We can relate $\mathbf{z}(t)$ to the model's state vector $\mathbf{b}(t)$ through the nonlinear observation equation

$$\mathbf{z} = \mathbf{h}(\mathbf{b}) + \mathbf{v}, \tag{14}$$

where $\mathbf{v}(t)$ represents uncorrelated measurement errors as a zero mean white noise process with known covariance $\mathbf{V}(t)$, i.e., $\mathbf{v}(t) \sim \mathbf{N}(\mathbf{0}, \mathbf{V}(t))$. If $\mathbf{z}$ consists of observations of time varying positions of model points at material coordinates u_k on the model's surface, the components of $\mathbf{h}$ are computed

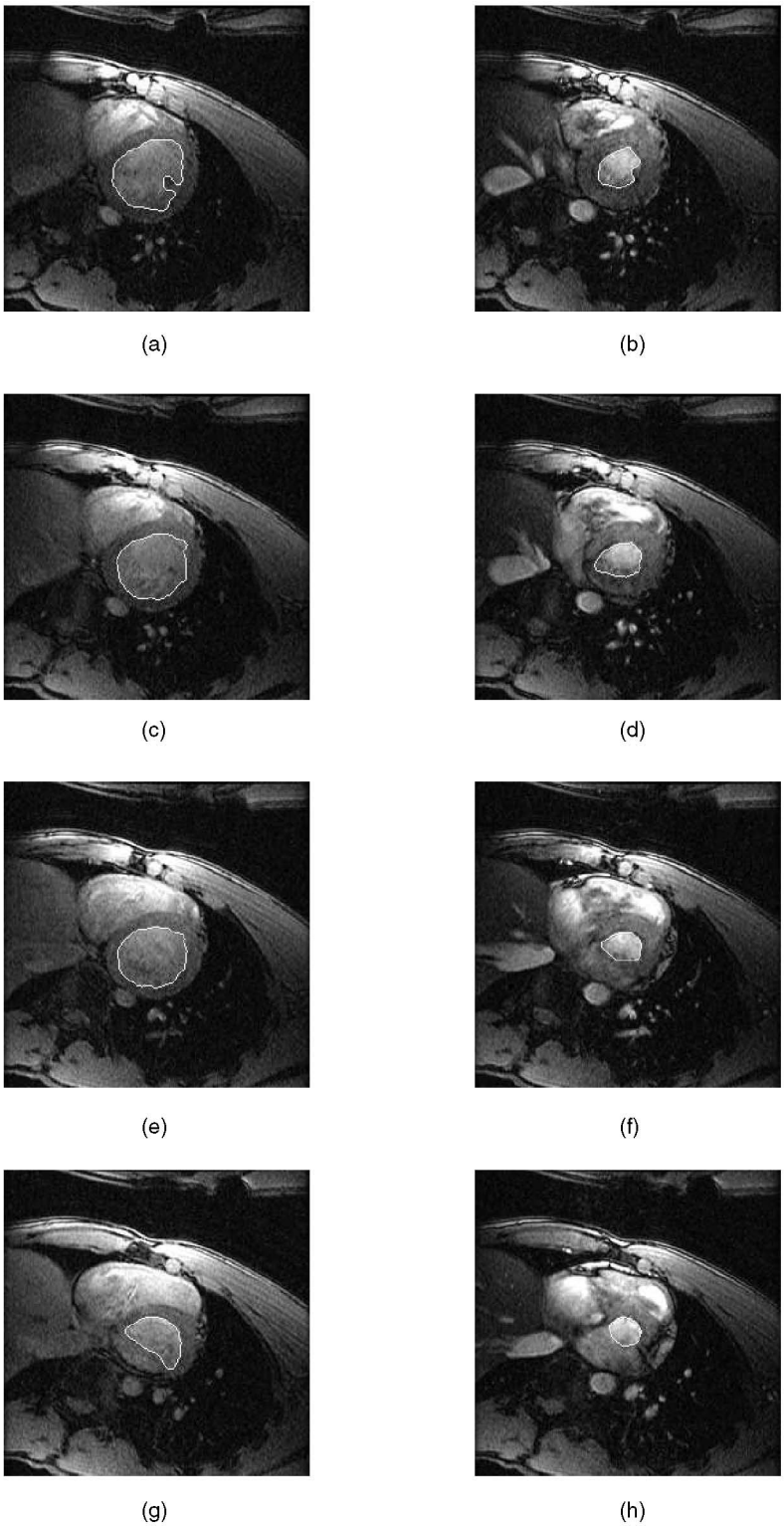

Fig. 3. Semiautomated identification of the myocardial borders. (a), (c), (e), and (g) End diastole phase and (b), (d), (f), and (h) end systole phase for locations 8, 9, 10, and 11, respectively.

using (1) evaluated at u_k [4] (see also [28]). In the case of computing an image potential, what is being measured at every node of the model is the difference $\mathbf{z} - \mathbf{h}(\mathbf{b})$, which is what is needed for an extended Kalman filter formulation. In addition, let us also assume that $\mathbf{a}(t)$ represents uncorrelated modeling errors as a zero mean white noise process with known covariance, i.e., $\mathbf{a}(t) \sim \mathbf{N}(\mathbf{0}, \mathbf{Q}(t))$.

Based on the above definitions and (4), the *modified* extended Kalman filter equations for our dynamic system take the following form:

4. Note that the definition of function $\mathbf{h}$ in (1) does not depend on $\mathbf{w}$.

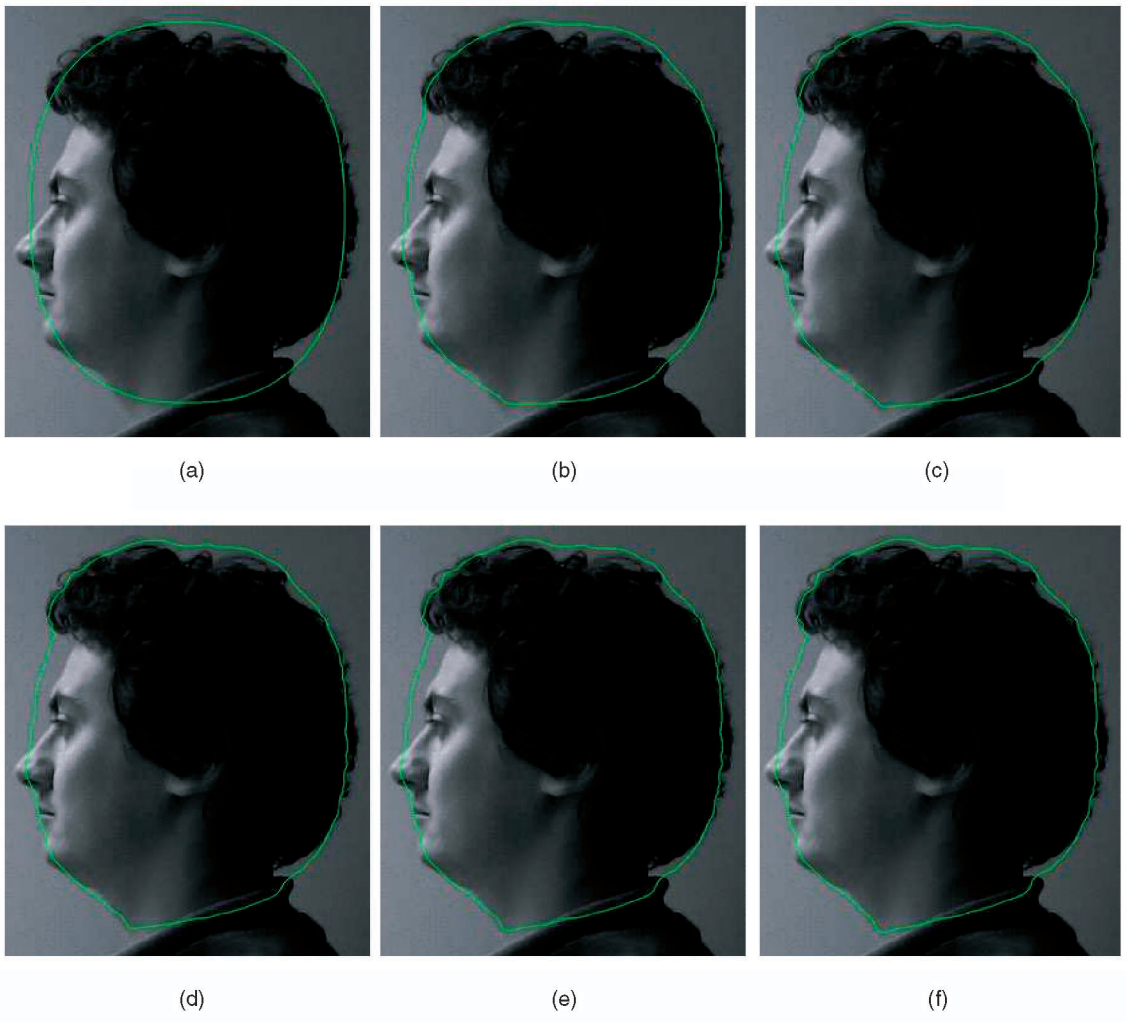

Fig. 4. Fitting the two-dimensional data from a subject's head using a nonelastically adaptive deformable model.

$$\dot{\mathbf{b}} = \mathbf{f}(\mathbf{b}) + \mathbf{a}, \tag{15}$$

$$\mathbf{z} = \mathbf{h}(\mathbf{b}) + \mathbf{v}, \tag{16}$$

where

$$\mathbf{f}(\mathbf{b}) = \begin{bmatrix} \dot{\mathbf{w}} \\ -\mathbf{K}\mathbf{q} \end{bmatrix}, \dot{\mathbf{w}} = \left(\dot{w}_1^1, \ldots, \dot{w}_i^j, \ldots, \dot{w}_6^k\right)^\top, \tag{17}$$

$$\dot{w}_i^j = (w_0 - w_{min})\ \ e^{sgn(\psi^j \cdot \dot{\psi}^j)(\|\psi^j\| + \|\dot{\psi}^j\|)} \\ sgn\left(\psi^j \cdot \dot{\psi}^j\right)\left[\frac{d}{dt}\left(\| \psi^j \|\right) + \frac{d}{dt}\left(\| \dot{\psi}^j \|\right)\right]. \tag{18}$$

Note that due to the modification in the state vector, we now have a fully nonlinear extended Kalman filter as opposed to our previous formulations [31]. However, the filter converges to the right solution since we impose a correct behavior onto the model for the adaptation of the model's elastic parameters and the model dynamics are appropriate for our applications.

The state estimation equation for uncorrelated system and measurement noises (i.e., $E[\mathbf{a}(t)\mathbf{v}^\top(t)] = 0$) is

$$\dot{\hat{\mathbf{b}}} = \mathbf{f}(\hat{\mathbf{b}}) + \mathbf{P}\mathbf{H}^\top\mathbf{V}^{-1}\left(\mathbf{z} - \mathbf{h}(\hat{\mathbf{b}})\right), \tag{19}$$

where $\mathbf{H}$ is computed from

$$\mathbf{H} = \left.\frac{\partial \mathbf{h}(\mathbf{b})}{\partial \mathbf{b}}\right|_{\mathbf{b}=\hat{\mathbf{b}}}. \tag{20}$$

The expression $\mathbf{G}(t) = \mathbf{P}\mathbf{H}^\top\mathbf{V}^{-1}$ is known as the Kalman gain matrix. The symmetric error covariance matrix $\mathbf{P}(t)$ is the solution of the matrix Riccati equation

$$\dot{\mathbf{P}} = \mathbf{F}\mathbf{P} + \mathbf{P}\mathbf{F}^\top + \mathbf{Q} - \mathbf{P}\mathbf{H}^\top\mathbf{V}^{-1}\mathbf{H}\mathbf{P}, \tag{21}$$

where

$$\mathbf{F}(\mathbf{b}) = \left.\frac{\partial \mathbf{f}(\mathbf{b})}{\partial \mathbf{u}}\right|_{\mathbf{b}=\hat{\mathbf{b}}}. \tag{22}$$

The improvement offered from the Kalman filter formulation is that one can formally introduce data noise statistics into the model.

5.1 Implementation

Since the model's equations of motion are numerically well-conditioned, the full Kalman filter formulated above can be partitioned into two separate filters for computational efficiency. The first filter includes the translation, rotation,

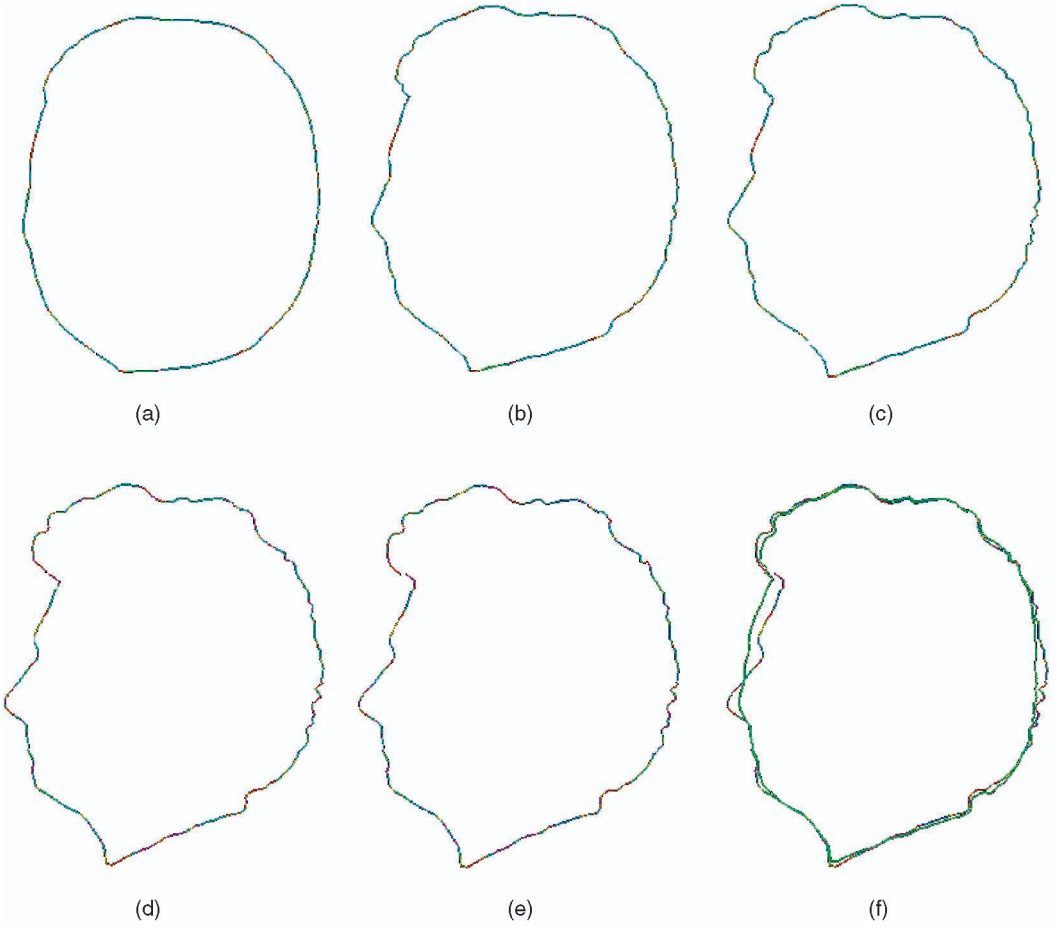

Fig. 5. (a), (b), (c), (d), and (e) Fitting the two-dimensional data from a subject's head using an elastically adaptive deformable model. (f) Comparison of the fitted shapes of the elastically adaptive and nonelastically adaptive models.

and global deformations, and the second one includes only the local deformations. While the computation to the solution of the Riccati equation for the first filter is fast since the associated degrees of freedom are few, this is not the case for the second filter whose state vector includes the model's elastic parameters and the local degrees of freedom.

To solve the matrix Riccati equations at interactive rates in the latter case, we take advantage of the decomposition of the model's surface into finite elements. A similar approach was used by Metaxas [28] for the computation of the stiffness matrix $\mathbf{K}$. Based on the covariance of each component of $\mathbf{u}$ that corresponds to the variable of the second Kalman filter at a given step, the contribution of each element to (22) is computed using the right hand side of this equation for each element. This per-element computation of (22) results in matrices of very small dimensions compared to the size of the respective matrices for the whole system. For example, in Experiment 3 (Section 6.3) we have deployed a deformable model with 902 nodes and 1,800 elements. Assuming a thin-plate deformation energy, this results in matrices of size 12×12 for the element by element approach and of size $16,212 \times 16,212$ for the whole system. Furthermore, this per-element computation can be done in parallel and once all the elements are looped through, the contribution from each element is placed at the appropriate location in $\mathbf{P}$ (in an identical way to the computation of $\mathbf{K}$). Then, we solve (22) [13]. This significantly improves the speed of the calculations (e.g., on average by 50 percent for models with 1,800 elements) and is justified since the model's surface is partitioned into finite elements. Of course, this speedup depends of the number of finite elements.

6 Results

Based on the above implementation, all our experiments ran at interactive rates on a Silicon Graphics R10000 Indigo^2 workstation with 256MB RAM. Furthermore, we always started from a unit covariance matrix $\mathbf{P}$. However, the subsequent structure of $\mathbf{P}$ was not diagonal and had a form similar to $\mathbf{K}$. Notice that any other reasonable initial condition will work if our dynamic model is appropriate for our applications. For the global deformations we used a superellipsoid or a superquadric, the elastic parameters were always initialized to $w_0 = 0.005$, $\mathbf{D} = \mathbf{I}$, and we used an adaptive Euler integration method for increased stability. Thus, in every iteration the model is getting closer to the data and the value of $\mathrm{sgn}(\boldsymbol{\psi}^j \cdot \boldsymbol{\psi}^{j})$ does not change between iterations. In addition, we defined $\mathbf{V}$ as $\mathbf{V} = 0.1\mathbf{I}$.

6.1 Experiment 1: Identification of the Myocardial Borders

In the first experiment, we applied our technique to the semiautomated identification of the myocardial borders from breath-hold MRI. The data was obtained from the Department of Radiology at the University of Pennsylvania. The data set included 16 slice locations, from the Left Ventricle

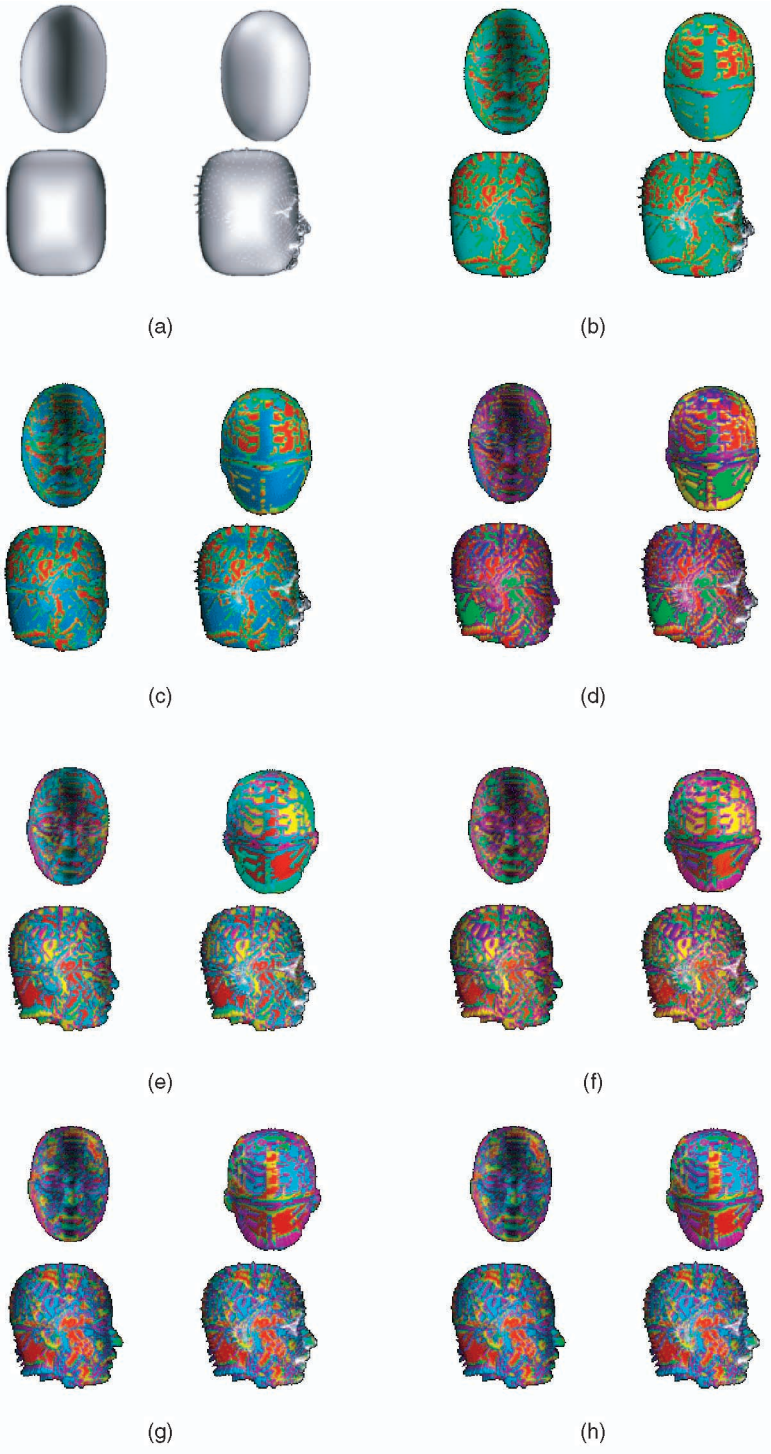

Fig. 6. Fitting the three-dimensional data.

(LV) apex to the level of the aortic valve. In order to determine the location of the borders with higher accuracy we magnified each image four times, and then we convolved it with an 8×8 Gaussian mask. An initial superellipsoid model (with 300 elements) was placed manually at the vicinity of the border of the first slice. In this study, we concentrated on the identification of the LV endocardial contour for locations 4 to 11 in which the contour is visible (Figs. 2 and 3). During the fitting process, the results from fitting one slice were used as the initial model for the next slice, as if we had an evolving curve over time. Therefore, the user only initialized the model in the first slice. Convergence was achieved in less than seven iterations (on average) for each slice. Figs. 2a, 2c, 2e, and 2g and Figs. 3a, 3c, 3e, and 3g depict the data from the end diastole phase at locations 4 through 11, respectively. Figs. 2b, 2d, 2f, and 2h and Figs. 3b, 3d, 3f, and 3h depict the data from the end systole phase at locations 4 through 11, respectively. The deformable models fitted to the myocardial borders are shown overlayed on the data.

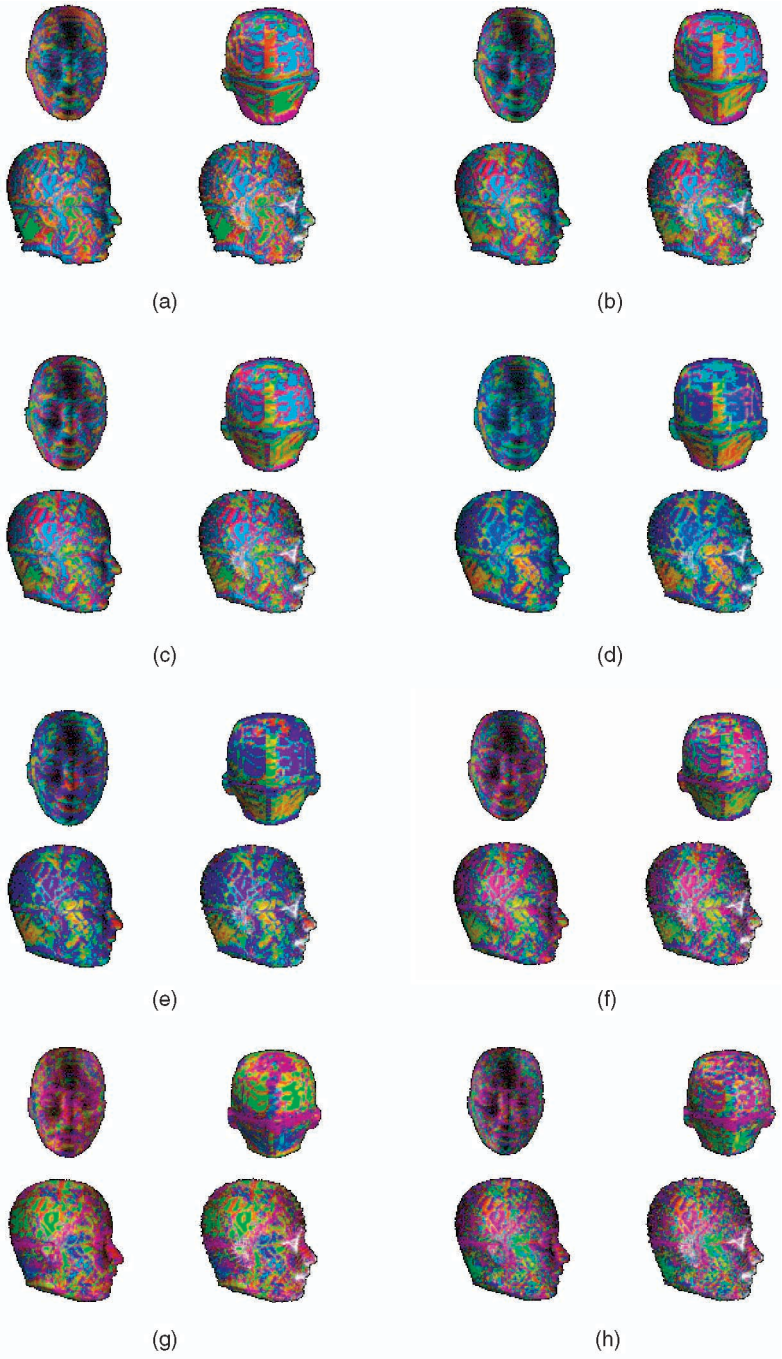

Fig. 7. Fitting the three-dimensional data (cont.).

6.2 Experiment 2: Two-Dimensional Shape Fitting

In this experiment, our goal was to fit the shape of the apparent contour of a subject's head. Figs. 4a, 4b, 4c, 4d, 4e, and 4f show the fitting evolution of a superellipsoid deformable model with $w = 0.005$ to the image data. In Fig. 4f, the model has reached an equilibrium state (after 20 iterations) and the fitting does not change over time. When the elastic parameters were automatically changed over time using our framework Figs. 5a, 5b, 5c, 5d, and 5e the result depicted in Fig. 5e was obtained (after eight iterations). This result can be compared to the result obtained using a nonelastically adaptive deformable model Fig. 5f.

6.3 Experiment 3: Three-Dimensional Shape Fitting

This experiment presents the fitting of an elastically adaptive deformable model to the 1,269 three-dimensional data points of a Viewpoint model of a human head. Each of the Figs. 6a, 6b, 6c, 6d, 6e, 6f, 6g, and 6h and Figs. 7a, 7b, 7c, 7d, 7e, 7f, 7g, and 7h is composed of four parts. The two subimages in the upper row of each subfigure depict the model as seen from the front and back, respectively. The lower left subimage of each figure depicts a side view of the model while the lower right subimage depicts the side view of the model along with the three-dimensional data. For example, the two subimages in the upper row of Fig. 6a depict the initial model from a frontal and a back view, respectively. The lower left subimage of each

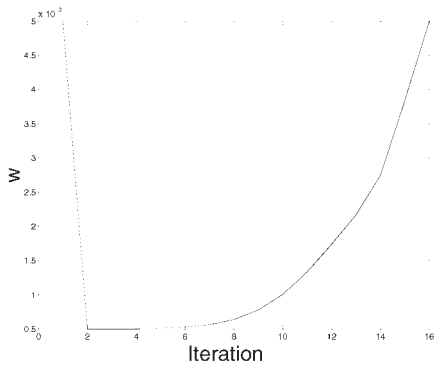

Fig. 8. Variation of the elastic parameters over time for the element 112 of the deformable model deployed for fitting the data from the head.

figure depicts a side view of the initial model while the lower right subimage depicts the side view of the model along with the three-dimensional data. In Figs. 6a, 6b, 6c, 6d, 6e, 6f, 6g, and 6h and Figs. 7a, 7b, 7c, 7d, 7e, 7f, 7g, and 7h, each finite element of the three-dimensional model is color-coded to depict the value of the elastic parameters at that time instant. Fig. 7h depicts the fitting result after 16 iterations.

7 Conclusion

In prior work on deformable model-based methods for shape estimation, researchers had to experimentally select the values for the elastic parameters to achieve accurate shape estimation results. This assumption implied that these values remained constant during the shape estimation, and more importantly these values had to be selected for each class of shapes that was to be fitted. We have presented a novel technique for the automatic adaptation of the values of a deformable model's elastic parameters. This technique obviates the need for careful elastic parameter initializations by the user and attains superior fitting results. However, our technique depends on the selection of w_{min}. It has been successfully applied to the identification of the myocardial borders from breath-hold MRI images, two-dimensional and three-dimensional data. This method, coupled with our method [30] for automatically adapting a model's nodes to better fit a given data set, provides a very promising approach towards automating the process of object shape estimation based on deformable models.

References

[1] A. Blake and M. Isard, "3D Position, Attitude and Shape Input Using Video Tracking of Hands and Lips," *Proc. SIGGRAPH '94, Ann. Conf. Series,* pp. 185-192, July 1994.

[2] A. Blake and A. Zisserman, *Visual Reconstruction.* Cambridge, Mass.: MIT Press, 1987.

[3] R.M. Bolle and B.C. Vemuri, "On Three-Dimensional Surface Reconstruction Methods," *IEEE Trans. Pattern Analysis and Machine Intelligence,* vol. 13, no. 1, pp. 1-13, Jan. 1991.

[4] T. Broida and R. Chellappa, "Estimation of Object Motion Parameters from Noisy Images," *IEEE Trans. Pattern Analysis and Machine Intelligence,* vol. 8, no. 1, pp. 90-98, Jan. 1986.

[5] A. Chakraborty, M. Worring, and J.S. Duncan, "On Multi-Feature Integration for Deformable Boundary Finding," *Proc. Fifth Int'l Conf. Computer Vision,* pp. 846-851, June 1995.

[6] L.D. Cohen, "On Active Contour Models and Balloons," *Computer Vision, Graphics and Image Processing: Image Understanding,* vol. 53, pp. 211-218, 1991.

[7] H. Delingette, "Simplex Meshes: A General Representation for 3D Shape Reconstruction," *Proc. IEEE Computer Soc. Conf. Computer Vision and Pattern Recognition,* pp. 856-859, June 1994.

[8] E.D. Dickmanns and V. Graefe, "Applications of Dynamic Monocular Machine Vision," *Machine Vision Applications,* vol. 1, pp. 241-261, 1988.

[9] P. Fua and C. Brechbuehler, "Imposing Hard Constraints on Deformable Models through Optimization in Orthogonal Subspaces," *Computer Vision and Image Understanding,* vol. 65, no. 2, pp. 148-162, 1997.

[10] A. Gelb, *Applied Optimal Estimation.* MIT Press, 1974.

[11] M.S. Grewal and A.P. Andrews, *Kalman Filtering: Theory and Applications.* Prentice Hall, 1993.

[12] W.C. Huang and D.B. Goldgof, "Adaptive-Size Meshes for Rigid and Nonrigid Shape Analysis and Synthesis," *IEEE Trans. Pattern Analysis and Machine Intelligence,* vol. 15, no. 6, pp. 611-616, June 1993.

[13] I.A. Kakadiaris, "Motion-Based Part Segmentation, Shape and Motion Estimation of Multi-Part Objects: Application to Human Body Tracking," PhD dissertation, Dept. of Computer Science, Univ. of Pennsylvania, Philadelphia, Oct. 1996.

[14] I.A. Kakadiaris and D. Metaxas, "3D Human Body Model Acquisition from Multiple Views," *Proc. Int'l Conf. Computer Vision,* pp. 618-623, June 1995.

[15] I.A. Kakadiaris and D. Metaxas, "3D Human Body Model Acquisition from Multiple Views," *Int'l J. Computer Vision,* vol. 30, no. 3, pp. 191-218, 1998.

[16] I.A. Kakadiaris and D. Metaxas, "Model-Based Estimation of 3D Human Motion," *IEEE Trans. Pattern Analysis and Machine Intelligence,* vol. 22, no. 12, pp. 1453-1459, 2000.

[17] I.A. Kakadiaris, D. Metaxas, and R. Bajcsy, "Inferring 2D Object Structure from the Deformation of Apparent Contours," *Computer Vision and Image Understanding,* vol. 65, no. 2, pp. 129-147, 1997.

[18] M. Kass, A. Witkin, and D. Terzopoulos, "Snakes: Active Contour Models," *Proc. Int'l Conf. Computer Vision,* pp. 259-268, June 1987.

[19] M. Kass, A. Witkin, and D. Terzopoulos, "Snakes: Active Contour Models," *Int'l J. Computer Vision,* vol. 1, no. 4, pp. 321-331, 1988.

[20] O.V. Larsen, P. Radeva, and E. Marti, "Bounds on the Optimal Elasticity Parameters for a Snake," *Proc. Eighth Int'l Conf. Image Analysis and Processing, ICIAP '95,* pp. 37-44, 1995.

[21] O.V. Larsen, P. Radeva, and E. Marti, "Guidelines for Choosing Optimal Parameters of Elasticity for Snakes," *Proc. Sixth Int'l Conf. Computer Analysis of Images and Patterns,* pp. 106-113, 1995.

[22] D. Lee and T. Pavlidis, "One Dimensional Regularization with Discontinuities," *IEEE Trans. Pattern Analysis and Machine Intelligence,* vol. 10, no. 6 pp. 822-829, 1988.

[23] C. Mandal, B.C. Vemuri, and H. Qin, "A New-Dynamic Fem-Based Subdivision Surface Model for Shape Recovery and Tracking in Medical Images," *Proc. Medical Image Computing and Computer-Assisted Intervention-MICCAI '98,* pp. 753-760, 1998.

[24] C. Mandal, B.C. Vemuri, and H. Qin, "Shape Recovery Using Dynamic Subdivision Surfaces," *IEEE Int'l Conf. Computer Vision,* pp. 805-810, Jan. 1998.

[25] L. Matthies, T. Kanade, and R. Szeliski, "Kalman Filter-Based Algorithms for Estimating Depth from Image Sequences," *Int'l J. Computer Vision,* vol. 3, no. 3, pp. 209-238, Sept. 1989.

[26] T. McInerney and D. Terzopoulos, "A Dynamic Finite Element Surface Model for Segmentation and Tracking in Multidimensional Medical Images with Application to Cardiac 4D Image Analysis," *Computerized Medical Imaging and Graphics,* vol. 19, no. 1, pp. 69-83, Jan. 1995.

[27] D. Metaxas, "Physics-Based Modeling of Nonrigid Objects for Vision and Graphics," PhD dissertation, Dept. of Computer Science, Univ. of Toronto, 1992.

[28] D. Metaxas, *Physics-Based Deformable Models: Applications to Computer Vision, Graphics and Medical Imaging.* Kluwer-Academic, 1996.

[29] D. Metaxas and I.A. Kakadiaris, "Elastically Adaptive Deformable Models," *Proc. Fourth European Conf. Computer Vision (ECCV),* vol. II, pp. 550-559, Apr. 1996.

[30] D. Metaxas, E. Koh, and N. Badler, "Multi-Level Shape Representation Using Global Deformations and Locally Adaptive Finite Elements," *Int'l J. Computer Vision,* vol. 25, no. 1, pp. 42-46, Oct. 1997.

[31] D. Metaxas and D. Terzopoulos, "Shape and Nonrigid Motion Estimation through Physics-Based Synthesis," *IEEE Trans. Pattern Analysis and Machine Intelligence,* vol. 15, no. 6, pp. 580-591, June 1993.

[32] J. Montagnat and H. Delingette, "Globally Constrained Deformable Models for 3D Object Reconstruction," *Signal Processing,* vol. 71, no. 2, pp. 173-186, Dec. 1998.

[33] A. Pentland and B. Horowitz, "Recovery of Non-Rigid Motion and Structure," *IEEE Trans. Pattern Analysis and Machine Intelligence,* vol. 13, no. 7, pp. 730-742, July 1991.

[34] A. Pentland and S. Sclaroff, "Closed-Form Solutions for Physically Based Modeling and Recognition," *IEEE Trans. Pattern Analysis and Machine Intelligence,* vol. 13, no. 7, pp. 715-729, July 1991.

[35] R. Samadani, "Adaptive Snakes: Control of Damping and Material Parameters," *Proc. SPIE Geometric Methods in Computer Vision,* no. 1570, 1991.

[36] S. Sclaroff and L. Liu, "Deformable Shape Detection and Description via Model-Based Region Grouping," *IEEE Trans. Pattern Analysis and Machine Intelligence,* vol. 23, no. 5, pp. 475-489, May 2001.

[37] D. Shen and C. Davatzikos, "An Adaptive-Focus Deformable Model Using Statistical and Geometric Information," *IEEE Trans. Pattern Analysis and Machine Intelligence,* vol. 22, no. 8, pp. 906-913, Aug. 2000.

[38] A. Singh, D. Goldgof, and D. Terzopoulos, *Deformable Models in Medical Image Analysis.* Los Alamitos, Calif.: IEEE CS, 1998.

[39] F. Solina and R. Bajcsy, "Recovery of Parametric Models from Range Images: The Case for Superquadrics with Global Deformations," *IEEE Trans. Pattern Analysis and Machine Intelligence,* vol. 12, no. 2, pp. 131-146, Feb. 1990.

[40] G. Sparr, "A Common Framework for Kinetic Depth, Reconstruction and Motion for Deformable Objects," *Proc. Third European Conf. Computer Vision,* pp. 471-482, May 1994.

[41] L.H. Staib and J.S. Duncan, "Boundary Finding with Parametrically Deformable Models," *IEEE Trans. Pattern Analysis and Machine Intelligence,* vol. 14, no. 11, pp. 1061-1075, Nov. 1992.

[42] D. Terzopoulos, "The Computation of Visible-Surface Representations," *IEEE Trans. Pattern Analysis and Machine Intelligence,* vol. 10, no. 4, pp. 417-438, Apr. 1988.

[43] D. Terzopoulos, "Regularization of Inverse Visual Problems Involving Discontinuities," *IEEE Trans. Pattern Analysis and Machine Intelligence,* vol. 8, no. 4, pp. 413-424, July 1986.

[44] D. Terzopoulos and D. Metaxas, "Dynamic 3D Models with Local and Global Deformations: Deformable Superquadrics," *IEEE Trans. Pattern Analysis and Machine Intelligence,* vol. 13, no. 7, pp. 703-714, July 1991.

[45] D. Terzopoulos, A. Witkin, and M. Kass, "Symmetry-Seeking Models and 3D Object Reconstruction," *Int'l J. Computer Vision,* vol. 1, no. 3, pp. 211-221, 1987.

[46] D. Terzopoulos, A. Witkin, and M. Kass, "Constraints on Deformable Models: Recovering 3D Shape and Nonrigid Motion," *Artificial Intelligence,* vol. 36, no. 1, pp. 91-123, 1988.

[47] M. Vasilescu and D. Terzopoulos, "Adaptive Meshes and Shells: Irregular Triangulation, Discontinuities, and Hierarchical Subdivisions," *Proc. IEEE Computer Soc. Conf. Computer Vision and Pattern Recognition,* pp. 829-832, June 1992.

[48] B.C. Vemuri and Y. Guo, "Pedal Snakes: Geometric Models with Physics-Based Control," *Proc. IEEE Int'l Conf. Computer Vision,* pp. 427-432, Jan. 1998.

[49] B.C. Vemuri, Y. Guo, S.H. Lai, and C.M. Leonard, "Fast Numerical Algorithms for Fitting Hybrid Shape Models to Brain MRI," *Medical Image Analysis,* vol. 1, no. 4 pp. 343-362, 1997.

[50] B.C. Vemuri and R. Malladi, "Constructing Intrinsic Parameters with Active Models for Invariant Surface Reconstruction," *IEEE Trans. Pattern Analysis and Machine Intelligence,* vol. 15, no. 7, pp. 668-681, July 1993.

[51] B.C. Vemuri and A. Radisavljevic, "Multiresolution Stochastic Hybrid Shape Models with Fractal Priors," *ACM Trans. Graphics,* vol. 13, no. 2, special issue on interactive sculpting, pp. 177-207, Apr. 1994.

[52] G. Wahba, *Spline Models for Observational Data.* SIAM, 1990.

[53] Y.F. Wang and J.F. Wang, "Surface Reconstruction Using Deformable Models with Interior and Boundary Constraints," *IEEE Trans. Pattern Analysis and Machine Intelligence,* vol. 14, no. 5, pp. 572-579, May 1992.

[54] R. Whitaker, "Algorithms for Implicit Deformable Models," *Proc. Fifth Int'l Conf. Computer Vision,* pp. 822-827, June 1995.

[55] G. Whitten, "Scale Space Tracking and Deformable Sheet Models for Computational Vision," *IEEE Trans. Pattern Analysis and Machine Intelligence,* vol. 15, no. 7, pp. 697-706, July 1993.

[56] C. Xu and J.L. Prince, "Generalized Gradient Vector Flow External Forces for Active Contours," *Signal Processing,* pp. 131-139, Dec. 1998.

[57] L. Zhou and C. Kambhamettu, "Extending Superquadrics with Exponent Functions: Modeling and Reconstruction," *Graphical Models and Image Processing,* vol. 63, no. 1, pp. 1-20, 2001.

[58] O. Zienkiewicz, *The Finite Element Method.* McGraw-Hill, 1977.

Dimitris N. Metaxas received the Diploma in electrical engineering from the National Technical University of Athens in 1986, the MSc degree in computer science from the University of Maryland in 1988, and the PhD degree in computer science from the University of Toronto in 1992. He is a professor in the Division of Computer and Information Science and the Department of Bioengineering at Rutgers University. From January 1998 to December 2001, he was an associate professor in the Department of Computer and Information Science at the University of Pennsylvania. From September 1992 to December 1997, he was an assistant professor in the same department. Dr. Metaxas is the director of the Center for Computarional Bioengineering, Imaging, and Modeling (CBIM) and while at PENN he was heading the Vision, Analysis and Simulation Technologies Lab (VAST). He specializes in physics-based techniques for the modeling, estimation and synthesis of the shape, and motion for complex objects. He is the author of the book *Physics-Based Deformable Models: Applications to Computer Vision, Graphics and Medical Imaging* published by Kluwer Academic Publishers in November 1996. He is an associate editor of *Graphical Models and Image Processing*, he is on the editorial board of *Medical Imaging*, and has been an associate editor for the *IEEE Transactions on Pattern Analysis and Machine Intelligence*. He has organized several workshops and conferences in his area, has served on the program committees of all major computer vision, medical imaging and computer graphics conferences since 1992, and has published more than 160 research publications in these areas. He received a US National Science Foundation Initiation Award (1993), a US National Science Foundation Career Award (1996), and a US Office of Naval Research Young Investigator Proposal Award (1997). He has been invited nationally and internationally to speak on his research and his research has received several best paper awards and patents. He has graduated 12 PhD students and is a member of ACM, IEEE Computer Society, and a senior member of the IEEE.

Ioannis A. Kakadiaris received the Ptychion (BS) degree (1989) in physics from the University of Athens, Greece, the MSc degree (1991) in computer science from the Northeastern University, Boston, Massachusetts, and the PhD degree (1997) in computer science from the University of Pennsylvania, Philadelphia. He has been an assistant professor in the Department of Computer Science at the University of Houston since August 1997. From November 1996 to July 1997, he was a postdoctoral fellow in the Department of Computer and Information Science at the University of Pennsylvania. He is the director of the UH Visual Computing Lab and director of the Division of Bioimaging and Biocomputation at the UH Center for Digital Informatics and Analysis. His research interests include computer vision, biomedical imaging, physics-based modeling and simulation, and multimodal human computer interaction. He received the US National Science Foundation Faculty Early Career Award in the Spring of 2000 and he has been elected to the IEEE Computer Society Distinguished Visitors Program 2002-2004. Dr. Kakadiaris is the focus group chair for Graphics and Visualization for the Computing Curricula 2001 and is a member of the ACM, IEEE, and the IEEE Computer Society.